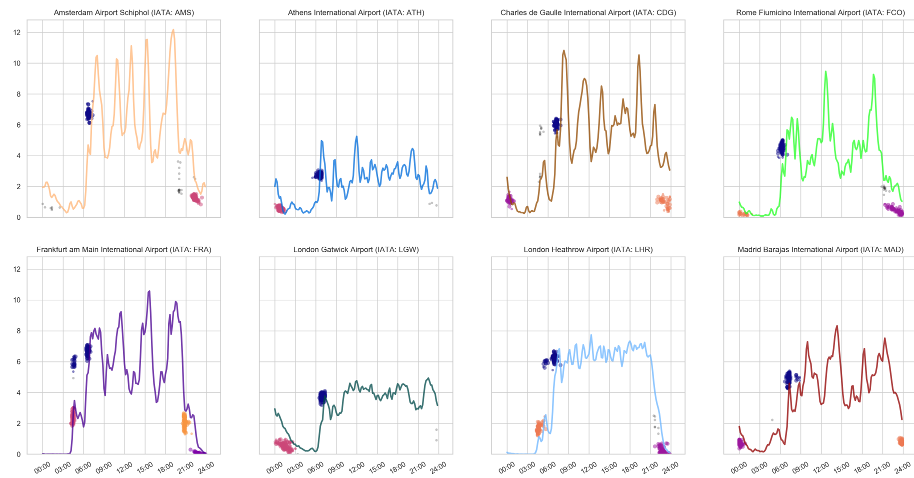

Figure A.1: Data-driven modeling of non-homogeneous Poisson process; MBIC penalty. DBSCAN outliers are drawn in black.

Supplementary material

Appendix A. PELT with MBIC and AIC penalty

This appendix offers a sensitivity analysis of the PELT algorithm with respect to the result of Algorithm 1. Figure A.1 shows the change-points identified by PELT and the resulting clustering via DBSCAN when PELT uses the default Modified Bayesian Information Criterion (MBIC) penalty. In this case, the change-points returned by PELT are so well-concentrated that the clustering step is barely needed. Accordingly, the number of outliers returned by DBSCAN (shown in black) is extremely limited. Identified clusters are limited in number and typically located early in the morning or late in the evening. Thus, the Poisson intensities returned by Algorithm 1 have a very straightforward interpretation as day and night regimes.

Figure A.2 shows the change-points identified by PELT and the resulting clustering via DBSCAN when PELT uses the Akaike Information Criterion (AIC) penalty. In this setting, PELT is much more sensible and detects regime changes in correspondence of maxima and minima of the average demand. The resulting description of the arrival stream in terms of a Poisson process is hence richer and

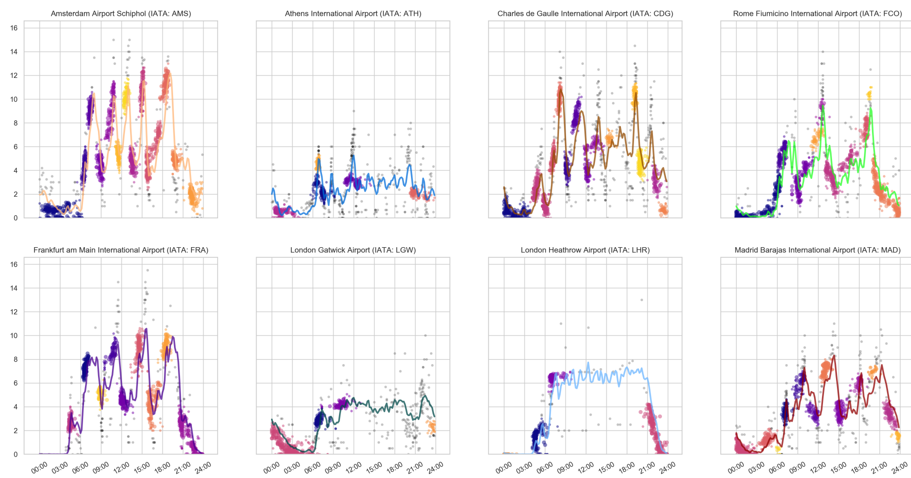

Figure A.2: Data-driven modeling of non-homogeneous Poisson process; AIC penalty. DBSCAN outliers are drawn in black.

follows more closely the average demand. However, the increased sensibility in the change point detection comes at the price of a *noisy* distribution of change-points in the (t, λ) plane, which might be difficult to reconstruct via DBSCAN (see LGW).

Appendix B. Continuous wavelet transform of demand time series

Figure B.3 shows a continuous wavelet transform of the demand from the week August 01–07, 2016. The x-axis shows the time and the y-axis shows the scale parameter of the Ricker wavelet. The color bar shows the value of the coefficients of the transform. The plot highlights the presence of a low-frequency component with daily periodicity and high-frequency demand peaks with sufficient regularity, the strength and frequency of which vary across airports.

Appendix C. Correlations from regulated flight plan and PSRA model

Figure C.4 shows the Pearson's correlation $\rho_{t_i,t_{i+1}}$ between the simulated demand variation in the intervals $[t_i, t_{i+1})$ and $[t_{i+1}, t_{i+2})$. The simulated demand variation is obtained by subtracting the demand according to the regulated flight plan t^r from the demand simulated from Model (3).

Comparing Figures 6 and C.4, we observe that the Pre-Scheduled Random Arrivals (PSRA) model (3) captures this characteristic of the inbound flow very well.

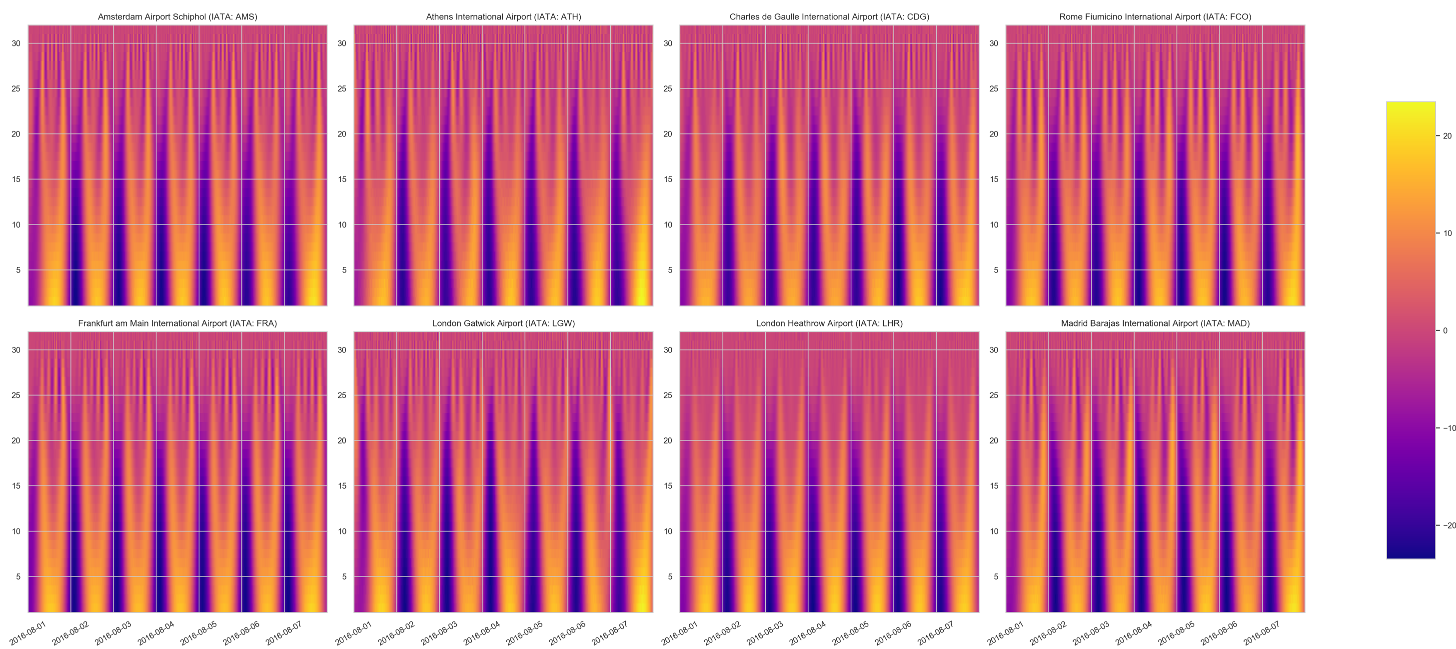

Figure B.3: Continuous wavelet transform of the demand for the week August 01–07, 2016. The figure clearly shows the presence of a weekly periodic component in the demand at all airports under consideration.

Figure C.4: Correlations from simulation of Model (3). Error bars show 95% confidence intervals for Pearson's ρ.

Appendix D. Intensity function of the data-driven Poisson process

This appendix details the intensity function of the Poisson process obtained in Section 3.3.1. The intensity function is a periodic right-continuous step-function, which takes on value $\hat{\lambda}$ between two consecutive values of $\hat{t}$. The values of $\hat{t}$ and $\hat{\lambda}$ are reported for each airport by Table D.1 below. The table shows how the model correctly captures the typical hourly landing rates in the moments of highest demand, when we expect the airport to operate close to its maximum capacity. For LHR, $\lambda = 0.64$ aircraft/min corresponds to 38.4 aircraft/hour, which is close to the maximum declared capacity of 45; for FRA, $\lambda = 0.90$ aircraft/min corresponds to 54 aircraft/hour, which is close to the maximum declared capacity of 60; finally, for AMS, $\lambda = 1.13$ aircraft/min corresponds to 67.8 aircraft/hour, which is very close to the the maximum declared capacity of 68 (capacity data from `https://ext.eurocontrol.int/airport_corner_public/`).

Table D.1: Non-homogeneous Poisson process derived by PELT and DBSCAN algorithms. The table reports the centroids of the clusters identified by DBSCAN and shown in Figure 7. Times are local.

airport	time	λ
FRA	04:32 UTC+02	0.2657 aircraft/min
	06:41 UTC+02	0.7325 aircraft/min
	08:55 UTC+02	0.4991 aircraft/min
	10:33 UTC+02	0.8550 aircraft/min
	12:14 UTC+02	0.4530 aircraft/min
	14:31 UTC+02	0.8757 aircraft/min
	16:31 UTC+02	0.4270 aircraft/min
	18:29 UTC+02	0.9034 aircraft/min
	22:04 UTC+02	0.1182 aircraft/min
LGW	02:40 UTC+01	0.0671 aircraft/min
	06:54 UTC+01	0.2858 aircraft/min
	10:10 UTC+01	0.4195 aircraft/min
	23:26 UTC+01	0.2328 aircraft/min
LHR	00:25 UTC+01	0.0000 aircraft/min
	04:56 UTC+01	0.1409 aircraft/min
	07:16 UTC+01	0.6410 aircraft/min
	22:24 UTC+01	0.1424 aircraft/min
AMS	02:47 UTC+02	0.0537 aircraft/min
	06:30 UTC+02	0.4222 aircraft/min
	07:25 UTC+02	0.9062 aircraft/min
	08:53 UTC+02	0.4416 aircraft/min
	10:28 UTC+02	0.9006 aircraft/min

Continued on next page

Table D.1 – *continued from previous page*

airport	time	λ
	11:30 UTC+02	0.5334 aircraft/min
	12:38 UTC+02	1.0207 aircraft/min
	13:35 UTC+02	0.4785 aircraft/min
	15:00 UTC+02	1.0653 aircraft/min
	16:23 UTC+02	0.5189 aircraft/min
	18:26 UTC+02	1.1255 aircraft/min
	19:52 UTC+02	0.4881 aircraft/min
	22:26 UTC+02	0.1942 aircraft/min
MAD	01:00 UTC+02	0.0386 aircraft/min
	04:30 UTC+02	0.1240 aircraft/min
	06:12 UTC+02	0.0293 aircraft/min
	07:14 UTC+02	0.3511 aircraft/min
	09:19 UTC+02	0.5870 aircraft/min
	11:18 UTC+02	0.3470 aircraft/min
	13:02 UTC+02	0.7084 aircraft/min
	15:14 UTC+02	0.3574 aircraft/min
	17:56 UTC+02	0.5905 aircraft/min
	20:01 UTC+02	0.6972 aircraft/min
	22:33 UTC+02	0.3309 aircraft/min
	23:35 UTC+02	0.1493 aircraft/min
CGD	01:24 UTC+02	0.0530 aircraft/min
	05:18 UTC+02	0.1852 aircraft/min
	07:08 UTC+02	0.5127 aircraft/min
	08:06 UTC+02	1.0003 aircraft/min
	09:11 UTC+02	0.4170 aircraft/min
	10:32 UTC+02	0.8515 aircraft/min
	12:11 UTC+02	0.3950 aircraft/min
	13:06 UTC+02	0.6116 aircraft/min
	15:29 UTC+02	0.6669 aircraft/min
	19:09 UTC+02	1.0227 aircraft/min
	20:01 UTC+02	0.4632 aircraft/min
	22:16 UTC+02	0.3120 aircraft/min
	23:21 UTC+02	0.0631 aircraft/min
ATH	01:27 UTC+03	0.0445 aircraft/min
	06:45 UTC+03	0.4592 aircraft/min
	07:16 UTC+03	0.2315 aircraft/min
	12:03 UTC+03	0.3028 aircraft/min
	21:27 UTC+03	0.1993 aircraft/min
FCO	03:29 UTC+02	0.1019 aircraft/min
	06:47 UTC+02	0.5395 aircraft/min
	09:24 UTC+02	0.3155 aircraft/min

Continued on next page

Table D.1 – *continued from previous page*

airport	time	λ
	11:49 UTC+02	0.6698 aircraft/min
	12:30 UTC+02	0.8899 aircraft/min
	14:48 UTC+02	0.3965 aircraft/min
	18:58 UTC+02	0.7465 aircraft/min
	19:31 UTC+02	1.0422 aircraft/min
	21:37 UTC+02	0.2130 aircraft/min